Neural circuit basis of adolescent THC-induced potentiation of opioid responses in adult mice

Elizabeth Hubbard[1#], Vivienne Mae Galinato[1#], Pieter Derdeyn[2#], Katrina Bartas[2], and Kevin T. Beier[1, 3-5*]

1 Department of Physiology and Biophysics, University of California, Irvine, Irvine, CA, USA 92697-4560

2 Program in Mathematical, Computational, and Systems Biology. University of California, Irvine, Irvine, CA, USA 92697-4560

3 Department of Neurobiology and Behavior, University of California, Irvine, Irvine, CA, USA 92697-4560

4 Department of Biomedical Engineering, University of California, Irvine, Irvine, CA, USA 92697-4560

5 Department of Pharmaceutical Sciences, University of California, Irvine, Irvine, CA, USA 92697-4560

Co-first authors

*Corresponding author

Contact information:

Kevin Beier

825 Health Sciences Road

Medical Sciences D337

Irvine, CA 92697

Phone: 949-824-1083

Email: kbeier@uci.edu

ABSTRACT:

Use of one drug of abuse typically influences the behavioral response to other drugs, either administered at the same time or a subsequent time point. The nature of the drugs being used, as well as the timing and dosing, also influence how these drugs interact. Here, we tested the effects of adolescent THC exposure on the development of morphine-induced behavioral adaptations following repeated morphine exposure during adulthood. We found that adolescent THC administration impacted morphine-induced behaviors across several dimensions, including potentiating reward and paradoxically impairing the development of morphine reward. We then mapped the whole-brain response to a reinstatement dose of morphine, finding that adolescent THC administration led to increased activity in the basal ganglia and increased functional connectivity between frontal cortical regions and the ventral tegmental area. Last, we show using rabies virus-based circuit mapping that adolescent THC exposure triggers a long-lasting elevation in connectivity from the frontal cortex regions onto ventral tegmental dopamine cells that has the potential to influence dopaminergic response to morphine administration during adulthood. Our study adds to the rich literature on the interaction between drugs of abuse and provides potential circuit substates by which adolescent THC exposure influences responses to morphine later in life.

INTRODUCTION:

Cannabis is currently the most widely used drug during adolescence in the United States[1]. Despite a reputation as a relatively harmless drug, over 30% of cannabis users meet the diagnostic criteria for cannabis use disorder (CUD)[2], a similar number as those who misuse psychoactive drugs such as cocaine and opioids[3]. With the trend of legalization across the globe enabling increased access to cannabis, it is critical to understand how adolescent cannabis use impacts the brain and behavior. Adolescent exposure to the major psychoactive constituent of cannabis, tetrahydrocannabinol (THC), has been linked to a variety of negative outcomes later in life[4–6], including increased consumption of psychoactive drugs[7–12]. Given the posited role of the mesolimbic dopamine system as the final common pathway for addiction[13], it is not surprising that brain regions such as the ventral tegmental area (VTA), medial prefrontal cortex (mPFC), and nucleus accumbens (NAc) are critically important in mediating the long-lasting effects of adolescent THC on responses to psychoactive drugs later in life[10,14–16]. Much like use of other psychoactive drugs[17–20], adolescent THC usage leads to a hyperdopaminergic state[15] that then facilitates a variety of neuroadaptations that promote addiction. Despite this common framework, our mechanistic understanding of how adolescent THC influences the adult brain is limited.

Given that THC carries an addictive liability, it is critically important to understand the interactions between adolescent THC usage and exposure to drugs of abuse later in life, for example prescription opioids. Despite the goal to reduce the clinical usage of opioids, opioids remain the primary treatment for post-operative pain management. Unfortunately, approximately eighty percent of those who use heroin

began using opioids for pain management[21,22]. As opioid exposure is thus in some cases largely unavoidable, it is important to understand how lifestyle factors such as adolescent THC usage influence response to opioids. In fact, the intersection of THC and opioids has been a question of substantial interest for many decades, in part due to the hypothesis that cannabis use may predispose individuals to opioid use[23–25]. This is supported by the observation that cannabinoids and opioids may both activate the midbrain dopamine system, perhaps via common mechanisms of mu opioid receptor activation[26]. Cross-sensitization of THC and morphine has been demonstrated[27], and adolescent THC exposure can alter expression of genes related to the endogenous opioid system[10], providing further evidence that these drugs may work via common mechanisms.

Here, we administer a moderate dose of THC (5 mg/kg) for 14 days starting at postnatal day 30 (PD30), during adolescence. We then test a variety of opioid-induced behaviors by administering morphine later in life and assess how adolescent THC administration influences these behaviors. We also assess how adolescent THC administration influences brain-wide activity patterns following a reinstatement dose of morphine, as well as how adolescent THC administration alters connectivity onto dopamine neurons in the VTA.

METHODS:

All procedures were approved by the University of California, Irvine's Institutional Animal Care and Use Committee (IACUC) and carried out in accordance with the National Institutes of Health guidelines for the care and use of animals. Adolescent male and female C57BL/6J mice were weaned and sexed at PD21 and group housed with same-sex littermates. Mice were housed in standard individually ventilated cages with corncob bedding and two cotton nestlets for enrichment. Lights were on a 12 hr on/12 hr off cycle (7:30-7:30) and rooms have controlled temperature (22ºC +/- 2ºC) and humidity (55-65%). Mice received ad libitum access to food and water.

.

<u>Adolescent THC Administration:</u> Mice were handled and weighed daily. On PD30, mice began daily injections of either 5 mg/kg THC or vehicle, which was composed of 5% Tween80 in saline. After 14 days of daily injections (PD30-PD43), mice were left in their home cage undisturbed (aside from weekly cage changes) until PD70 when behavioral testing began.

<u>Drugs:</u> THC was provided by the NIDA Drug Supply Program or Cayman Chemicals (Ann Arbor, MI) and administered at 5 mg/kg. Morphine was purchased from Patterson and was administered at 10 mg/kg.

<u>Behavioral Testing:</u>

Locomotion: The distance traveled in the open field was assessed during 30-minute recording sessions. Open field boxes were outfitted with contexts to differentiate them from the open field test for anxiety. Locomotion was assessed once per day for seven days, the first two following saline injections for habituation days, and the last five following injection of 10 mg/kg morphine. Mice were excluded if data from >1 day of the task were missing.

Conditioned place preference: Custom two chamber acrylic boxes separated by a small corridor with distinct visual contexts on the walls of each side were used for CPP tests. On the pre-test day, mice were placed in the box with no barriers and were allowed to freely explore both sides for 30 minutes, and the time spent in each chamber was recorded. Following the pre-test, mice underwent two saline pairings and two morphine pairings. In the morning, the mice were given saline and paired with the preferred chamber, and in the afternoon, injected with morphine and paired with the non-preferred chamber. Control mice received saline in both contexts. On the post-test day, mice were again placed in the CPP chamber with no barriers, and the amount of time spent in each chamber was recorded. Data were plotted as the relative time spent on the drug-paired chamber in the post-test relative to the pre-test. Mice were subject to exclusion if the time spent on one side during the CPP pretest was less than 600 seconds or more than 1200 seconds.

Elevated plus maze: Mice were placed at the end of one of the open arms, facing outwards. Mice were then able to freely explore the maze for 5 minutes, and the time spent in the open arms was recorded. Tests were performed in dim lighting ~25 lux.

Open field test: Mice were placed in a 40cm x 40cm square arena made of opaque plexiglass and were able to freely explore during a 5-minute test. During analysis, the arena was divided into nine equal square zones. The time spent in the center square for each mouse was calculated. Tests were performed under bright lighting conditions of ~1000 lux.

Marble burying: Mice were placed in a rat cage with 20 marbles placed on top of corn-cob bedding. After 30 minutes, the number of marbles that were buried by each mouse was recorded. Withdrawal tests were not performed on one cohort of mice.

Von Frey: The von Frey test was used to assess mechanical sensitivity. Mice were placed on top of a wire mesh platform, restrained underneath a glass beaker, and allowed to acclimate for at least 30 minutes. The mouse's right hindpaw was gently touched with different filaments, starting with the 0.4g filament. If the mouse showed a withdrawal response (such as lifting, shaking, or licking the paw), the experimenter stepped down to a lighter filament, and if the mouse did not respond, the experimenter

130 stepped up to a thicker filament until a response occurred. The process continued with filaments of higher
131 or lower forces for four additional turns following the first change in response. This up/down method was
132 used to determine the mechanical force required to elicit a paw withdrawal response in 50% of animals[28].
133
134 cFos induction and immunohistochemistry: One hour following injection of 5 mg/kg morphine, mice were
135 perfused with PBS followed by 4% formaldehyde, and brains isolated and post-fixed overnight in 4%
136 formaldehyde. The following day, brain clearing began using iDISCO[29]. The monoclonal rat anti-cFos
137 antibody (Synaptic Systems lot #226017) in 5% NDS/PBS-Tween 0.1% was used at a 1:5000 dilution,
138 with an incubation time of five days. Donkey anti-rat Cy3 (Jackson Immunoresearch) was then used at a
139 dilution of 1:250. Brains were then cleared in dibenzyl ether and imaged using a Zeiss Z1 light-sheet
140 microscope. Accurate detection of cFos+ neurons was ensured by manual quality control checks for each
141 brain. ClearMap[30] was then used to align the imaged brains to the Allen Brain Reference Atlas, and to
142 quantify the cFos+ neurons in anatomically-defined brain regions.
143
144 Network Analysis: Anatomical projection data from the Allen Mouse Brain Connectivity Atlas was used to
145 construct a connectivity matrix among the brain regions in our analysis[31]. This atlas quantifies axonal
146 arborization from AAV injections to measure projections from one region to another. The density of each
147 projection, or the sum or projecting pixels dividing by the total pixels in that region, was normalized by
148 dividing by the volume of injection, so as not to bias experiments with more virus injection than others.
149 This quantity was also multiplied by the number of voxels in the injection structure to avoid
150 overrepresentation of smaller regions. This quantity was computed for every pair of source and target
151 regions to build a connectivity matrix. We log-normalized these quantities so that they would have a more
152 normal distribution and behave better in network analysis. Community detection was performed using
153 the Louvain algorithm with a resolution parameter of 1, in the scit-kit network library[32]. Once the clusters
154 were determined, the cFos fold change of their regions were compared using a one-way ANOVA followed
155 by pairwise t-tests.
156
157 Functional Analysis: Regional cFos counts across each mouse in the adolescent vehicle-treated and
158 THC-treated conditions were dimensionally reduced using UMAP, so that regions with similar counts
159 across the mice would be embedded close to each other[33]. Regions were clustered using HDBSCAN,
160 which can identify hierarchical clusters in continuous data based on variations in density of the data[34].
161 Hierarchical clustering was also performed on the correlations between regions, to look more closely at
162 their functional relationships. R^2 value from Pearson correlations were computed for each pair of regions,
163 based on their counts across mice of a given condition. Hierarchical clusterings were computed on
164 correlation matrices using the average linkages methodology. For visualizations, the hierarchical
165 clustering tree was cut at a height of 0.75 to determine the clusters (Figure 4I-J). The trees were cut for

166 heights between 0.5 and 1 to observe trends in modularity across the two conditions. The seaborn library
167 was used for all hierarchical clustering computations[35].
168
169 Rabies virus circuit mapping: Rabies virus (RABV) monosynaptic tracing studies were carried out as
170 previously described[19,36], with minor modifications. On Day 0, 100 nL of a 1:1 volume mixture of AAV-
171 CAG-FLEx^{loxP}-TC and AAV-CAG-FLEx^{loxP}-G was injected into the VTA of PD56 mice that had undergone
172 two weeks of THC injections between PD30 and PD43. Fourteen days later, RABV was injected into the
173 VTA. After recovery, mice were housed in a BSL2 facility for 5 days to allow RABV spread and GFP
174 expression. Mice were then perfused with PBS followed by 4% formaldehyde and postfixed overnight.
175 Fixed brains were cryoprotected by incubation in a 30% sucrose solution overnight, and frozen in OCT.
176 Brains were then serially sliced on a cryostat into 60 um sections. GFP+ cells throughout the brain in 22
177 anatomically-defined input sites were counted manually, as previously performed[19,36].
178
179 Viruses and injection coordinates: Coordinates used for the VTA were (relative to Bregma, midline, or
180 dorsal brain surface and in mm): AP − 3.20, ML 0.4, DV − 4.2.
181
182 The titers of viruses, based on quantitative PCR analysis, were as follows:
183 AAV-CAG-FLEx^{loxP}-TC, serotype 5, 2.4 x 10^{13} genome copies (gc)/ml
184 AAV-CAG-FLEx^{loxP}-G, serotype 8, 1.0 x 10^{12} gc/ml
185
186 For RABV, the titer was performed on HEK 293T-TVA800 cells.
187 RABV (EnvA-pseudotyped, GFP-expressing), 5.0 x 10^{8} colony forming units (cfu)/ml.
188
189 After scaling RABV data, PCA was applied so features were brain regions and observations were
190 individual brains of mice treated with various drugs. Differences between mouse brains were
191 visualized by plotting PC1, PC2, and PC3 (Figure 5J-L, Q-R). Ellipsoids for each condition were
192 calculated and overlayed onto plots to visualize trends in PC values by condition. To further quantify
193 relationships between brains and conditions, the Euclidean distance between each point (or each
194 brain) in the PC1 versus PC2 coordinate space was calculated. These distances were then plotted
195 in a heatmap with brains being organized by similarity assessed by hierarchical clustering (Figure
196 5M). Alternatively, for a summary by condition, these distances were averaged based on drug
197 administered, and the resulting heatmap and clustering were made based on averaged Euclidean
198 distance values (Figure 5S). Heatmaps and clustering were made using the clustermap function in
199 the Python package seaborn with default parameters[35].
200

Quantification and Statistical Analysis: Statistics for all were calculated using GraphPad Prism 9 software. Statistical significance between direct comparisons was assessed by unpaired or paired t-tests. When multiple conditions were compared, one- or two-way ANOVAs were first performed, as appropriate, then t-tests were then performed for each individual comparison. Multiple comparisons corrections were performed when multiple such t-tests were being performed, and significance was assessed using the Holm-Bonferroni method. In conditions where multiple comparisons were performed and the results were still considered significant, asterisks were presented corresponding to the original p-values. Paired t-tests were used in cases with repeat measurements. Dot plots presented throughout the manuscript include a bar representing the mean value for each group. Error bars represent s.e.m. throughout. For all figures, ns $P > 0.05$, * $P \leq 0.05$, ** $P \leq 0.01$, *** $P \leq 0.001$, **** $P \leq 0.0001$.

RESULTS:

Adolescent THC exposure reduces morphine-induced locomotion, with no impact on morphine reward when given during young adulthood

We first exposed mice to a daily 5 mg/kg/day dose of THC during adolescence, here defined as postnatal days 30-43 (Figure 1A). This is considered a moderate dose that is mildly aversive and anxiogenic[37]. Animals receiving daily injections of vehicle on equivalent days were used as controls. Following vehicle or THC administration, mice were left in their home cages undisturbed besides weekly cage changes until postnatal day 70, at which time behavioral testing commenced. The protocol of morphine administration and behavioral testing is shown in Figure 1B. To test how adolescent THC exposure may impact morphine reward, we performed a two-dose morphine conditioned place preference (CPP) using 10 mg/kg morphine (Figure 1C). We induced a significant preference to the morphine-paired side in both vehicle and THC exposed animals, to an approximately equivalent extent, whereas no preference was observed in animals treated with vehicle during adolescence and again at adulthood in place of morphine (Vehicle/saline 762s pre, 778s post, $p = 0.22$; Vehicle/morphine 783s pre vs. 887s post, $p = 0.038$; THC/morphine 785s pre vs. 887s post, $p = 0.0017$; Figure 1D). To determine whether adolescent THC treatment impacted morphine-induced locomotion, we measured locomotor behavior while mice were in an open field. Following a two-day habituation protocol where mice were given saline injections, 10 mg/kg morphine was given once per day for five days (Figure 1E). We observed that adolescent THC exposure blunted morphine-induced locomotion during the five-day morphine administration window (RM Two-way ANOVA $p = 0.045$; Figure 1F), though no individual day was significantly different between the groups following multiple comparisons corrections. These data indicate that adolescent THC exposure reduced morphine-induced locomotion following morphine exposure later in life.

Adolescent THC exposure impairs the development of anxiety-related behavior and pain hypersensitivity during morphine withdrawal.

We next assessed whether mice treated with THC during adolescence were differentially impacted by withdrawal from repeated morphine administration. Following the five days of morphine given for locomotor testing and two days for CPP extinction, mice were left in their home cages for an additional 8 days, for a total abstinence period of ten days (Figure 2A). Following this ten-day forced abstinence, mice were tested for anxiety-like behavior using three tests: the elevated plus maze, open field test, and marble burying tests. The elevated plus maze tests how mice balance their tendency to explore against their preference for enclosed spaces (Figure 2B). A reduction in the time spent exploring the open arms is interpreted as an anxiety-like behavior. Mice treated with repeated morphine injections spent less time in the open arms of the elevated plus maze relative to those treated with repeated saline injections. However, adolescent THC exposure blocked the reduction in time spent in the open arms induced by repeat morphine injection (One-way ANOVA $p = 0.0005$; pairwise t-tests, vehicle/saline vs. vehicle/morphine 47.73s vs. 17.84s, $p = 0.01$; vehicle/saline vs. THC/morphine 47.73s vs. 42.39s, $p = 0.67$; vehicle/morphine vs. THC/morphine 17.84s vs. 42.39s, $p = 0.0018$; Figure 2C). Similar results were observed using the open field test, where mice are both compelled to explore new environments, and avoid open areas (Figure 2D). Less time spent exploring the center of the arena is interpreted as anxiety-like behavior. We found that repeat morphine injections reduced time spent in the center of the open field, and THC reduced this anxiety-like behavior (One-way ANOVA $p = 0.027$; pairwise t-tests, vehicle/saline vs. vehicle/morphine 22.66s vs. 12.55s, $p = 0.030$; vehicle/saline vs. THC/morphine 22.66s vs. 15.85s, $p = 0.077$; vehicle/morphine vs. THC/morphine 12.55s vs. 15.85s, $p = 0.59$; Figure 2E). Finally, in the marble burying test mice tend to bury marbles that are exposed in the bedding of a new cage (Figure 2F). In this assay, more marbles buried is interpreted to reflect increased anxiety-like behavior. We found that mice undergoing forced abstinence following repeat morphine injections buried more marbles after the 30-minute test, whereas adolescent THC administration reduced this number, consistent with an elevated anxiety-like behavior (One-way ANOVA $p = 0.0006$; pairwise t-tests, vehicle/saline vs. vehicle/morphine 0.93 vs. 3.67, $p = 0.0048$; vehicle/saline vs. THC/morphine 0.93 vs. 0.50, $p = 0.83$; vehicle/morphine vs. THC/morphine 3.67 vs. 0.50, $p = 0.006$; Figure 2G). Therefore, the results from each of these tests support the conclusion that adolescent THC exposure decreases the expression of anxiety-like behaviors in morphine-treated mice.

Next, we used a von Frey assay to examine the effects of adolescent THC exposure on mechanical hypersensitivity, both before and after morphine injection (Figure 2H). Mice treated with repeated THC doses during adolescence showed no difference in mechanical thresholds when tested one day prior to morphine CPP testing (Vehicle/morphine vs. THC/morphine 0.85g vs 0.86g, $p = 0.93$; Figure 2I). However, when tested again following repeat morphine exposure and forced abstinence, mice given repeated morphine administration showed an increased mechanical hypersensitivity relative to saline-treated controls, and adolescent THC treated reduced the extent of this hypersensitivity (One-way ANOVA p =

273 0.0032; pairwise t-tests, vehicle/saline vs. vehicle/morphine 1.09g vs. 0.42g, p = 0.0027; vehicle/saline
274 vs. THC/morphine 1.09g vs. 0.69g, p = 0.052; vehicle/morphine vs. THC/morphine 0.42g vs. 0.69g, p =
275 0.30; Figure 2J). Together, these results indicate that adolescent THC exposure reduces the expression
276 of morphine withdrawal-induced behaviors following repeated morphine administration during adulthood.
277
278 **Adolescent THC exposure enhances drug-induced reinstatement of morphine CPP**
279 Following forced abstinence, we next assessed whether mice differentially reinstated CPP following a 5
280 mg/kg exposure of morphine in the CPP box. Drug exposure following abstinence can reinstate
281 previously extinguished drug-seeking behaviors, and therefore can serve as a model of relapse in mice.
282 Mice showed normal CPP (e.g., Figure 1D) and the majority extinguished normally following 2 extinction
283 sessions (Figure 3A-B). To reduce confounding factors while examining reinstatement, mice were
284 excluded that did not show normal CPP or CPP extinction. While mice treated with vehicle during
285 adolescence did not significantly reinstate CPP following the priming 5 mg/kg morphine injection using
286 this protocol, mice treated with THC during adolescence did significantly reinstate their CPP
287 (Vehicle/morphine-treated mice 722s vs 801.3s, = p = 0.43; THC/morphine treated mice 780.7s vs. 1015s,
288 p = 0.027; Figure 3C). This means that adolescent THC exposure drives reinstatement of drug-seeking
289 behavior in mice in response to a sub-threshold dose of morphine in mice given vehicle during
290 adolescence.
291
292 **Whole-brain analysis shows differences in brain activity following drug-primed**
293 **reinstatement in adolescent vehicle- vs. THC-treated mice**
294 Given that adolescent THC-treated mice showed a more robust drug-primed reinstatement than vehicle-
295 treated mice, we next assessed what neural pathways may be responsible for this effect. To do this, we
296 perfused the mice 60 minutes following the reinstatement test, cleared the brains using iDISCO+, and
297 immunostained for the immediately early gene cFos to obtain a brain-wide map of neuronal activity
298 (Figure 4A). We observed an overall elevation of neuronal activity in mice treated with THC during
299 adolescence than vehicle, as evidenced by a higher number of cFos+ cells upon morphine exposure
300 (Figure 4B). This increase was exhibited in most brain regions, with some of the highest-fold elevations
301 occurring in basal ganglia regions including the globus pallidus externus (GPe), subthalamic nucleus
302 (STN) and substantia nigra pars reticulata (SNr), as well as areas such as the substantia
303 innominate/ventral pallidum, and several thalamic regions (Figure 4B-D). In fact, only four brain regions
304 showed a reduction in cFos labeling in adolescent THC-treated mice, which included both the medial and
305 lateral habenula.
306
307 As the elevation in cFos labeling occurred globally in the mouse brain, we wanted to assess whether this
308 elevation was larger for some pathways or whether the activation was uniform. To test this, we built a

309 quantitative connectivity matrix of the mouse brain, using the Allen Mouse Brain Connectivity Atlas as a
310 template[31]. Doing so revealed the existence of four major network communities within the brain, largely
311 consisting of subcortical regions including the VTA (community 1, purple), cortical regions (community 2,
312 blue), the hippocampus and related connections (community 3, red), and mid/hindbrain regions
313 (community 4, yellow) (Figure 4E). We then assessed the relative increase in cFos labeling of regions in
314 each community in adolescent THC- vs. vehicle-treated mice following a reinstatement opioid dose. We
315 found a significant increase in the log fold-change cFos labeling in the purple and blue communities
316 relative to the yellow community, suggesting that the subcortical and cortical modules both showed an
317 overall larger increase in activity relative to mid/hindbrain regions in THC-treated mice (Figure 4F).
318
319 Following this analysis, we wanted to assess if these pathway-specific changes in cFos activation were
320 accompanied by any changes in the functional relationships of different brain regions. To do so, we took
321 the cFos labeling data across all regions for all mice and performed a dimensionality reduction analysis
322 using Uniform Manifold Approximation and Projection (UMAP). UMAP divided the brain regions into
323 approximately 10 activity-defined clusters in the adolescent THC-treated mice data, clusters which
324 mapped relatively consistently onto the adolescent vehicle-treated mice data (Figure 4G-H), with some
325 increased spread in brains from vehicle-treated compared to THC-treated mice. Interestingly, while
326 frontal cortex regions, including the mPFC subregions infralimbic cortex (IL), prelimbic cortex (PL),
327 anterior cingulate cortex (ACC), and anterior insula cortex (AI) all were in relatively close proximity in
328 UMAP space in both adolescent vehicle-treated mice and THC-treated mice, they clustered much more
329 tightly together in THC-treated group relative to the vehicle-treated group, indicating a higher level of
330 correlated activity following a reinstatement opioid exposure (Figure 4G-H), suggesting that adolescent
331 THC exposure may increase the functional connectivity between frontal cortex regions and the VTA. To
332 assess functional modularity more quantitatively, we built a brain-wide functional correlation matrix for
333 adolescent THC-treated and vehicle-treated mice based on their cFos labeling (Figure 4I-J). While in
334 vehicle-treated mice the VTA and frontal cortex regions separated into different clusters, reflecting their
335 separation into different networks (Figure 4I), in THC-treated mice the IL, PL, ACC, and AI all co-clustered
336 with the VTA, indicating a higher level of correlated activity amongst these regions in adolescent THC-
337 treated mice (Figure 4J). Last, we wanted to assess the overall modularity of brain activity in adolescent
338 THC- vs. vehicle-treated mice. To do this, we determined the number of unique clusters across a range
339 of parameters. Across a wide parameter range, adolescent THC-treated mice exhibited fewer activity-
340 defined clusters than vehicle-treated mice, reflecting an overall reduced modularity in brains from
341 adolescent THC-treated mice (Figure 4K). These findings overall show that the increased activation of
342 cortical and subcortical pathways in adolescent THC-treated vs vehicle-treated mice after reinstatement
343 is accompanied by a collapse in modularity of pathways in adolescent THC-treated mice, including a
344 tighter clustering of the VTA with frontal cortex regions.

345

346 **Adolescent THC exposure changes connectivity to ventral tegmental area dopamine cells**

347 VTA is a critical brain region for the development of a variety of drug-induced behavioral adaptations,
348 including drug reward, sensitization, and withdrawal. To test whether adolescent THC exposure modified
349 the input control to VTA dopamine (VTA^{DA}) cells, we mapped inputs to these cells using the rabies virus
350 (RABV) monosynaptic input mapping method. First, in animals treated with THC during adolescence,
351 Cre-dependent adeno-associated viruses (AAVs) expressing TVA and the RABV glycoprotein, RABV-G,
352 were injected into the VTA of DAT-Cre mice. Two weeks later, mice were injected with a glycoprotein-
353 deleted, EnvA-pseudotyped, GFP-expressing RABV (Figure 5A). This virus infected TVA-expressing
354 cells by nature of the EnvA-TVA interaction. Once in VTA^{DA} cells, this virus could spread to their inputs,
355 as RABV-G was expressed in DAT-Cre cells. However, once in input cells, since RABV did not express
356 its own glycoprotein, the virus could not spread further. Five days later, experiments were terminated,
357 and GFP-positive cells were counted throughout the brain as we did previously[19,38], and input connectivity
358 was assessed. RABV-labeled input cells were observed throughout the brain, as in previous studies
359 (Figure 5B-C). Overall, we observed several quantitative differences, quantified in Figure 5D (Two-way
360 ANOVA, interaction $p = 0.0062$). While several brain regions showed a visible difference in connectivity,
361 for example elevated connectivity from the anterior cortex, parabrachial nucleus (PBN) and deep
362 cerebellar nuclei (DCN), only the anterior cortex was significantly different following correction for multiple
363 comparisons (corrected p-value $p = 0.029$).

364

365 This traditional approach to assessing differences in connectivity is statistically conservative, and only
366 assesses potential differences in connectivity, one input at a time. To reveal further patterns in the data,
367 we have recently employed a dimensionality reduction approach that enables us to detect larger-scale
368 differences in input patterns between brains of mice undergoing a variety of treatments[38,39]. We therefore
369 first used this approach to assess which inputs best differentiated THC-treated vs. control mice using
370 principal component analysis (PCA). We found that 3 PCs were sufficient to explain approximately 75%
371 of the variance in the data, and thus we focused only on these 3 PCs (Figure 5E-F). We found that PC1
372 completely separated THC-treated and control mice, whereas PC2 and PC3 did not (Figure 5G-I). Control
373 mice had high PC1 values, which were driven predominately by strong contributions from nucleus
374 accumbens medial shell (NAcMed), core (NAcCore), ventral pallidum (VP), septum, lateral habenula
375 (LHb) and medial habenula (MHb), while THC-treated mice had low PC1 values, which were driven by
376 the bed nucleus of the stria terminalis (BNST), extended amygdala area (EAM), entopeduncular nucleus
377 (EP), paraventricular nucleus of the hypothalamus (PVH), lateral hypothalamus (LH), and PBN (Figure
378 5G). To quantify these differences, we plotted each brain's location on each PC, and performed t-tests.
379 Differences between THC-treated and control groups were strongly significant along PC1, and not
380 different along PCs 2 and 3, as expected (Control 3.3 vs. THC -2.2, $p = 0.0002$). To further quantify

381 relationships between brains and conditions, the Euclidean distance between each brain in the PC1
382 versus PC2 coordinate space was calculated, and the relationships plotted as a correlogram. THC-
383 treated and control brains separated largely by condition, as expected (Figure 5M).
384
385 Last, we assessed how VTA^{DA} connectivity of THC-treated mice compares to mice treated with one of
386 several drugs, including a single dose of the psychoactive but non-addictive fluoxetine, two doses of the
387 anesthetic mixture of 100 mg/kg ketamine and 10 mg/kg xylazine, spaced 2 weeks apart, or one dose of
388 the addictive cocaine, amphetamine, methamphetamine, morphine, or nicotine, together grouped as
389 drugs of abuse. Using a similar PCA-based assessment, we observed that mice treated with a drug of
390 abuse separated from the other conditions along PC2, but not PC1 or PC3 (Figure 5N-P). Interestingly,
391 THC-treated mice had even higher values of PC2 than mice treated with one of the drugs of abuse and
392 were thus located further along PC2 from controls (Figure 5O-P). Positive values of PC2 were largely
393 driven by strong contributions from the anterior cortex, BNST, EP, CeA, LH, PBN, and DCN, notably
394 many of the same regions that differentiated brains of THC-treated from controls (Figure 5G, N). While
395 PC3 did not strongly differentiate most of the groups, it did differentiate THC-treated mice from those
396 treated with a drug of abuse (Figure 5R). THC-treated mice had higher PC3 values, which were driven
397 by strong contributions from the anterior cortex, dorsal striatum (DStr), PVH, CeA, PBN, and DCN (Figure
398 5N). The locations of each brain in PC space were plotted on bar graphs, and differences were again
399 assessed (PC2; Saline vs. THC -2.43 vs. 2.96, $p < 0.0001$; Fluoxetine vs. THC -1.55 vs. 2.96, $p = 0.0004$;
400 K/X vs. THC -1.23 vs. 2.96 $p = 0.0024$; Drugs vs. THC 0.19 vs. 2.96, $p = 0.0051$. PC3; One-way ANOVA
401 $p = 0.0004$; Saline vs. THC 0.70 vs. 1.85, $p = 0.63$; Fluoxetine vs. THC 0.88 vs. 1.85, $p = 0.71$; K/X vs.
402 THC 0.19 vs. 1.85 $p = 0.27$; Drugs vs. THC -0.79 vs. 1.85, $p = 0.0005$; Figure 5Q-R). The distinct
403 connectivity patterns were also apparent following our Euclidean distance analysis in PC1 and PC2 space,
404 which indicated that the connectivity patterns from brains from THC-treated mice segregate completely
405 from those of mice treated with other psychoactive drugs (Figure 5S). Together, these results indicate
406 that adolescent THC treatment induces similar but distinct input changes onto VTA^{DA} neurons, principally
407 an increase in connectivity from the anterior cortex.
408
409 **DISCUSSION**:
410 Here, we tested the effects of adolescent THC exposure on morphine-induced behaviors later in life, and
411 consequences for brain-wide activity following reinstatement and midbrain dopamine cell connectivity.
412 We found that adolescent THC exposure influences morphine responses across a variety of behavioral
413 dimensions, including locomotion, withdrawal-induced anxiety-related behavior, pain hypersensitivity,
414 and reinstatement. This broad range of effects is consistent with findings from studies that have explored
415 the influence of THC on morphine-induced behavioral changes, and vice versa[40,41]. Here, we extend
416 these previous studies by linking brain-wide activity patterns following a reinstatement dose of morphine

417 to morphine-induced reinstatement behavior and show that adolescent THC exposure creates long-
418 lasting changes in input connectivity to VTA^{DA} cells, which has the potential to alter the dopaminergic
419 response to morphine administration later in life. Our study thus adds to a rich literature on the subject
420 by implicating several discreet circuits as potential drivers of the long-lasting behavioral effects induced
421 by adolescent THC exposure on responses to opioids later in life.
422
423 While adolescent THC exposure enhances the behavioral response to a reinstatement dose of morphine,
424 consistent with adolescent THC potentiating behavioral responses to morphine, it is perhaps surprising
425 that THC exposure blunts morphine withdrawal-induced anxiety and pain. Interestingly, behavioral profile
426 is consistent with the behavioral responses observed following exposure of drugs of abuse during
427 adolescence[42–46], where adolescent mice experience potentiated drug reward with only mild withdrawal
428 symptoms relative to adult mice receiving equivalent drug exposures. This effect could be mediated by
429 an occlusion of opioid-induced epigenetic changes by those elicited following adolescent THC exposure.
430 Such an effect was previously observed following juvenile exposure to oxycodone; in this case,
431 oxycodone induced long-lasting epigenetic changes, for example an elevation of the repressive histone
432 modification H3K27me3 on genes that control dopamine transmission in the VTA[47]. Therefore, one
433 hypothesis is that adolescent THC exposure may result in a similar imbalance of reward/aversion as is
434 seen in responses to drugs during adolescence by occluding compensatory responses to drug exposure
435 that typically occur in adulthood, but not adolescence. In this case, reversal of these epigenetic marks
436 may restore mice to basal levels of susceptibility. Future studies are required to identify the potential
437 cellular loci of these effects, as well as what the epigenetic consequences of each life THC exposure
438 may be.
439
440 In addition, we found that adolescent THC administration induces higher levels of drug-induced
441 reinstatement, consistent with previous observations assessing drug- or stress-induced
442 reinstatement[8,9,41]. Here, we extend these observations by linking these results to brain-wide cFos
443 activation in adolescent vehicle- vs. THC-treated mice. Overall, we found that adolescent THC-treated
444 mice had higher numbers of cFos+ cells in response to a 5 mg/kg reinstatement dose of morphine than
445 adolescent vehicle-treated controls. In addition, we found that adolescent THC-treated mice have higher
446 levels of correlated activity in mPFC and AI regions with the VTA than adolescent vehicle-treated mice,
447 indicating enhanced connectivity between these regions (Figure 4G-H). We previously showed that
448 activation of these cortical inputs to the VTA promotes reinforcement through increasing dopamine
449 release in the NAc[36]. Therefore, the elevated functional connectivity that we observe between these
450 regions in adolescent THC-treated mice may promote greater levels of dopamine release in the NAc than
451 in adolescent vehicle-treated mice and is one mechanism by which adolescent THC-treated mice may
452 more strongly reinstate morphine CPP following a priming dose of morphine.

453

454 However, one limitation of cFos-based analyses is that they do not consider anatomical connections.
455 Viral methods such as the monosynaptic RABV circuit mapping technique can specifically label
456 synaptically-connected cells[48,49]. Furthermore, we recently showed that the extent of input labeling is
457 dependent on the activity of input connections[19,20,50]. Therefore, our RABV mapping experiments have
458 the unique ability to explore the changes in connectivity to VTA^{DA} cells following repeated THC exposure,
459 without a preconceived bias as to which inputs may be altered. We have previously used this assay to
460 define how drugs of abuse change inputs to VTA^{DA} cells, enabling us to identify several pathway-specific
461 changes that have important consequences for the development of drug-induced behavioral
462 adaptations[38]. Here, we compare connectivity of VTA^{DA} cells in brains from mice receiving our adolescent
463 THC protocol to those receiving a single drug of abuse. We found that adolescent THC exposure induced
464 numerous long-lasting input changes onto VTA^{DA} cells that partially, but not completely, overlapped with
465 those induced by a drug of abuse. The most prominent difference between mice given adolescent THC
466 exposure vs. a drug of abuse is that THC-treated mice show a pronounced increase in inputs from the
467 anterior cortex (Figure 5D). Heightened activation of this connection is consistent with our cFos results
468 and would be expected to be rewarding through elevating activity in VTA^{DA} cells. This hypothesis is
469 consistent with the hyper-dopaminergic state of THC-treated animals previously reported[15], and the more
470 robust response in these animals to a reinstatement dose of morphine.

471

472 In our study, we also tested the hypothesis that adolescent THC exposure alters connectivity onto VTA
473 dopamine (VTA^{DA}) cells. This hypothesis was supported by the observation that rats treated with THC
474 during adolescence develop a hyper-dopaminergic state[15]; one potential mechanism that could mediate
475 this effect would be a change in connectivity to facilitate an increase in DA release in downstream brain
476 regions. Here, we found an elevation in inputs from the anterior cortex to VTA^{DA} cells, which we previously
477 showed promotes reinstatement by facilitating DA release in the NAc. Notably, we previously have shown
478 that a single injection of a variety of drugs of abuse can cause long-lasting changes in input connectivity
479 onto VTA^{DA} cells[19,20,50], with this signature being relatively similar regardless of the drug administered[19,38],
480 suggesting that these drugs induce similar changes in connectivity. Interestingly, in those studies we did
481 not observe an increase in inputs from the anterior cortex[19,20,38,50]. In fact, inputs from the anterior cortex
482 tend to be depressed following drug administration[19], and this reduction was one of the three brain regions
483 that showed a significant change in connectivity following drug administration. The anterior cortex,
484 particularly the mPFC, is thought to play important roles in the later stages of substance use disorder[51–
485 54]. The reduction in connectivity following a single dose, and increase in connectivity following repeated
486 doses, is thus consistent with that hypothesis of increased mPFC engagement later in the addiction cycle.
487 One additional point of note is that we previously showed that drugs of abuse increase connectivity from
488 the globus pallidus externus (GPe) to the ventral midbrain, and that these changes are important for drug-

489 induced behavioral adaptations including reward and sensitization[19,20]. However, THC treatment did not
490 induce a notable change in GPe inputs onto VTA^{DA} cells (Figure 5D). Thus, while THC triggers several
491 long-lasting changes in connectivity to VTA^{DA} cells, these appear to be distinct from those initiated by
492 psychostimulants, nicotine, or morphine. However, the conclusions that we can draw from these
493 experiments are limited by differences in experimental design. For example, for the drug-treated mice,
494 RABV was injected one day following injection of the drug, whereas in THC-treated mice, they were
495 injected approximately 35 days following completion of a 2-week daily injection protocol. Thus, while in
496 the former study design drug-induced changes do not need to persist for longer than a few days to yield
497 the observed changes, in THC-treated animals the effects observed had to persist for longer than 35
498 days. In addition, THC was given fourteen times, once per day, whereas all other drugs were only given
499 once in total. Therefore, the effects observed with THC may result from repeated injections. However,
500 we performed the experiments presented here because our behavioral assessments were done 35 days
501 following completion of THC administration, and we wanted the RABV experiments to follow the same
502 timeline. Further experiments will be needed to resolve these questions.
503
504 **Acknowledgements:** We would like to thank Dr. Daniele Piomelli and the Impact of Cannabinoids
505 Across the Lifespan team at the University of California, Irvine for providing seed funding for this work.
506 This work was additionally funded by the NIH (R00 DA041445, DP2 AG067666, R01NS130044,
507 R01DA056599, 1R01DA054374), Tobacco Related Disease Research Program (T31KT1437,
508 T31P1426), One Mind (OM-5596678), Brightfocus Foundation (A2022031S), and the Brain and Behavior
509 Research Foundation (NARSAD 26845) to KTB, T32 GM136624 to KB and PD, NSF GRFP DGE-
510 1839285 to PD, and NIH T32 DA050558 to EH.

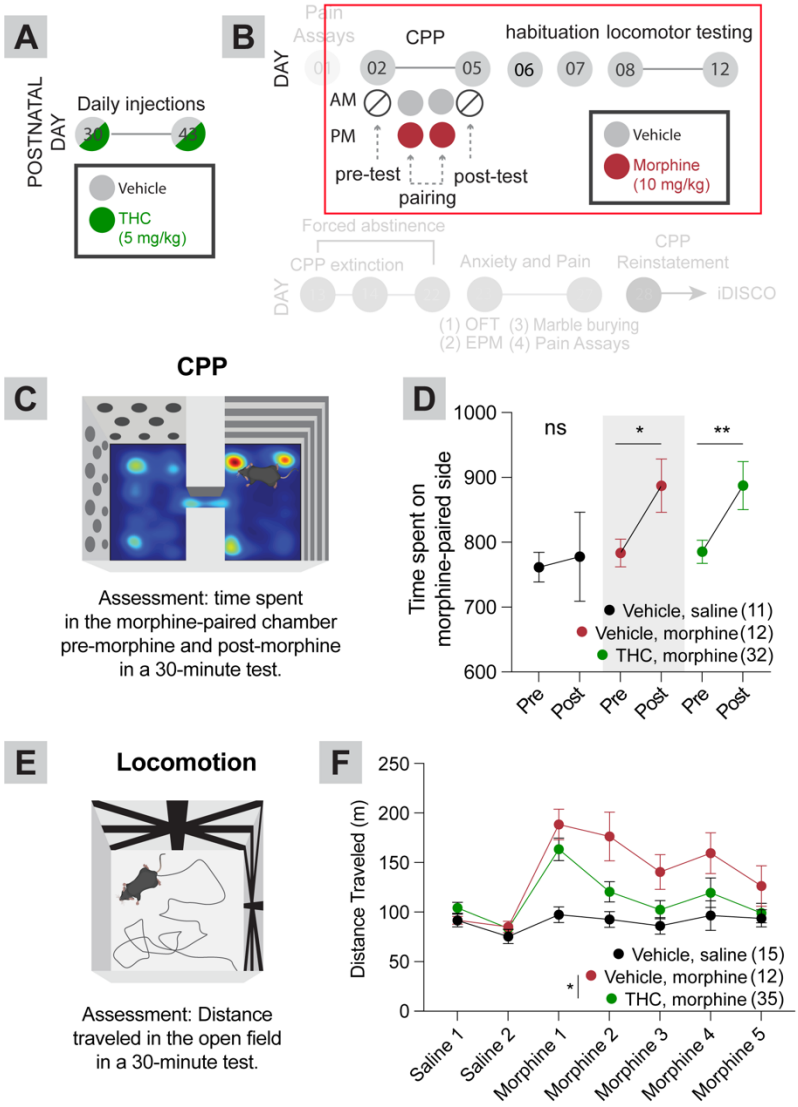

FIGURES:

Figure 1: Effects of adolescent THC exposure on behavioral responses to morphine administration later in life.

A, Timeline of THC or vehicle injections during adolescence. Injections were repeated once per day for 14 total days.

B, Morphine injections, and behavioral testing. The entire protocol is shown for each of Figures 1-3 for reference, with the relevant tests presented in the figure in full opacity and surrounded by red boxes.

C, Schematic of the conditioned place preference test.

D, Time spent in the morphine-paired chamber in the pre-test and post-test (in the vehicle/saline-paired group, both chambers were paired with saline). Vehicle/saline 762s pre, 778s post, $p = 0.22$; Vehicle/morphine 783s pre vs. 887s post, $p = 0.038$; THC/morphine 785s pre vs. 887s post, $p = 0.0017$.

E, Schematic of the locomotor test.

F, Mice treated with THC during adolescence showed an overall reduction in morphine-induced locomotion relative to mice treated with saline during adolescence. Repeat measures Two-way ANOVA between conditions $p = 0.045$; Sidak's multiple comparisons tests morphine day 1 $p = 0.68$, morphine day 2 $p = 0.24$, morphine day 3 $p = 0.31$, morphine day 4 $p = 0.50$, morphine day 5 $p = 0.75$. Vecchio/saline-treated mice are shown for comparison but were not included in statistical tests. Two-way ANOA only included morphine injection days, not habituation days. For this and all figures, error bars = SEM, ns $p > 0.05$, * $p < 0.05$, ** $p < 0.01$, *** $p < 0.001$, **** $p < 0.0001$.

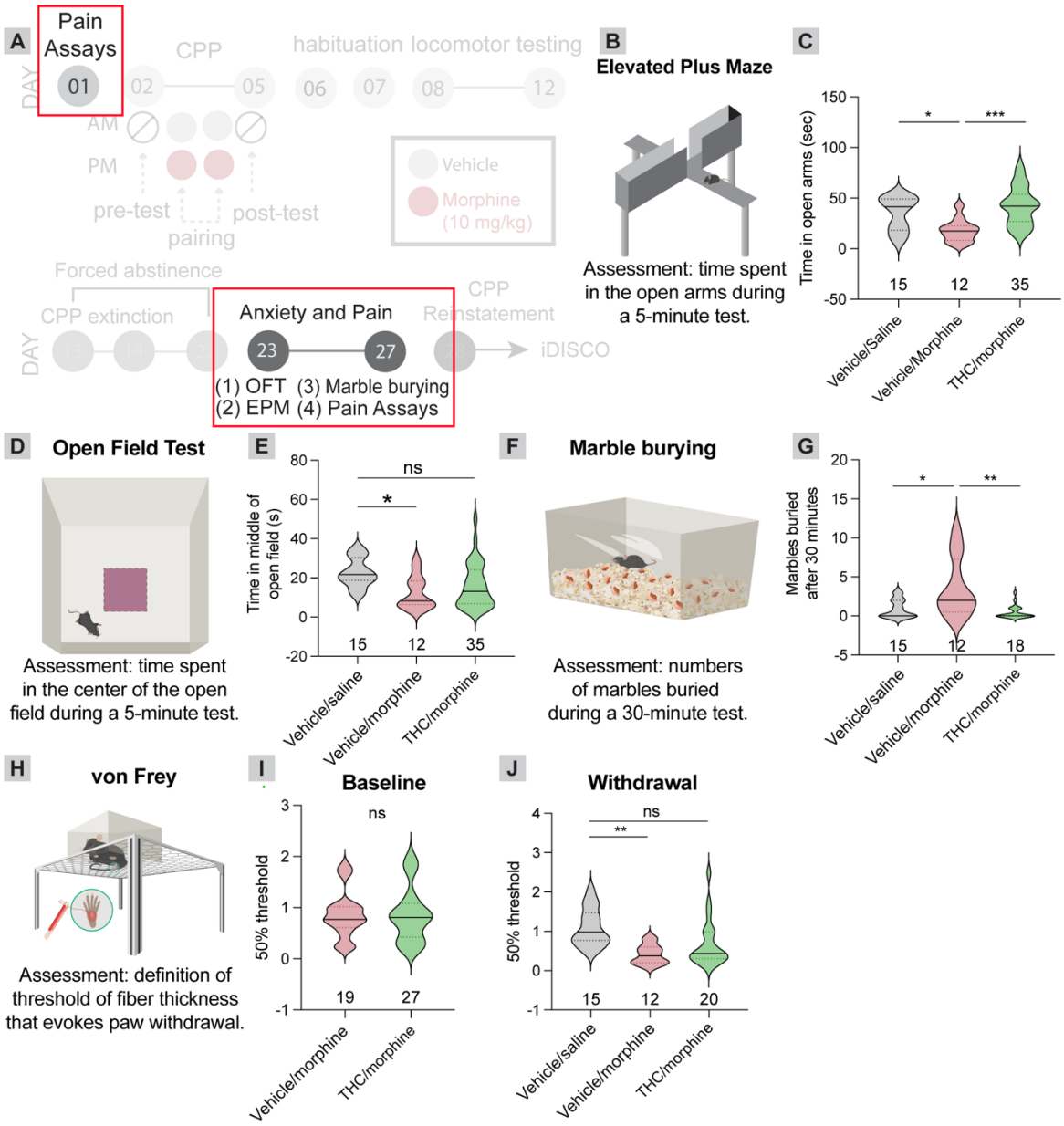

Figure 2: Adolescent THC administration reduces expression of morphine-induced withdrawal behaviors during a prolonged abstinence period.

A, Timeline of experiments.

B, Schematic of the elevated plus maze test.

C, Repeated morphine administration leads to a reduction in the time spent in the open arms of an elevated plus maze, indicative of anxiety-like behavior relative to mice treated with saline during adolescence, and saline during adulthood. Adolescent THC exposure prevented this morphine-induced anxiety. One-way ANOVA p = 0.0005; pairwise t-tests, vehicle/saline vs. vehicle/morphine 47.73 s vs. 17.84 s, p = 0.01; vehicle/saline vs. THC/morphine 47.73 s vs. 42.39 s, p = 0.67; vehicle/morphine vs. THC/morphine 17.84 s vs. 42.39 s, p = 0.0018.

D, Schematic of the open field test.

E, Repeated morphine administration leads to a reduction in the time spent in the center of an open field relative to mice treated with saline during adolescence, and saline during adulthood. Adolescent THC exposure blunted this reduction. One-way ANOVA $p = 0.027$; pairwise t-tests, vehicle/saline vs. vehicle/morphine 22.66 s vs. 12.55 s, $p = 0.030$; vehicle/saline vs. THC/morphine 22.66 s vs. 15.85 s, $p = 0.077$; vehicle/morphine vs. THC/morphine 12.55 s vs. 15.85 s, $p = 0.59$.

F, Schematic of the marble burying task.

G, Repeated morphine administration leads to an elevation in the number of marbles buried, indicative of anxiety-like behavior relative to mice treated with saline during adolescence, and saline during adulthood. Adolescent THC exposure prevented this morphine-induced anxiety. One-way ANOVA $p = 0.0006$; pairwise t-tests, vehicle/saline vs. vehicle/morphine 0.93 vs. 3.67, $p = 0.0048$; vehicle/saline vs. THC/morphine 0.93 vs. 0.50, $p = 0.83$; vehicle/morphine vs. THC/morphine 3.67 vs. 0.50, $p = 0.006$.

H, Schematic of the von Frey task of mechanical hypersensitivity.

I, Mice given saline vs. THC during adolescence showed no difference in baseline mechanical sensitivity. Vehicle/morphine vs. THC/morphine 0.85 g vs 0.86 g, $p = 0.93$. **J**, Repeated morphine administration leads to a reduction in the 50% mechanical threshold, indicative of pain hypersensitivity relative to mice treated with vehicle during adolescence, and saline during adulthood. Adolescent THC exposure blunted this morphine-induced pain hypersensitivity. One-way ANOVA $p = 0.0032$; pairwise t-tests, vehicle/saline vs. vehicle/morphine 1.09 vs. 0.42, $p = 0.0027$; vehicle/saline vs. THC/morphine 1.09 vs. 0.69, $p = 0.052$; vehicle/morphine vs. THC/morphine 0.42 vs. 0.69, $p = 0.30$.

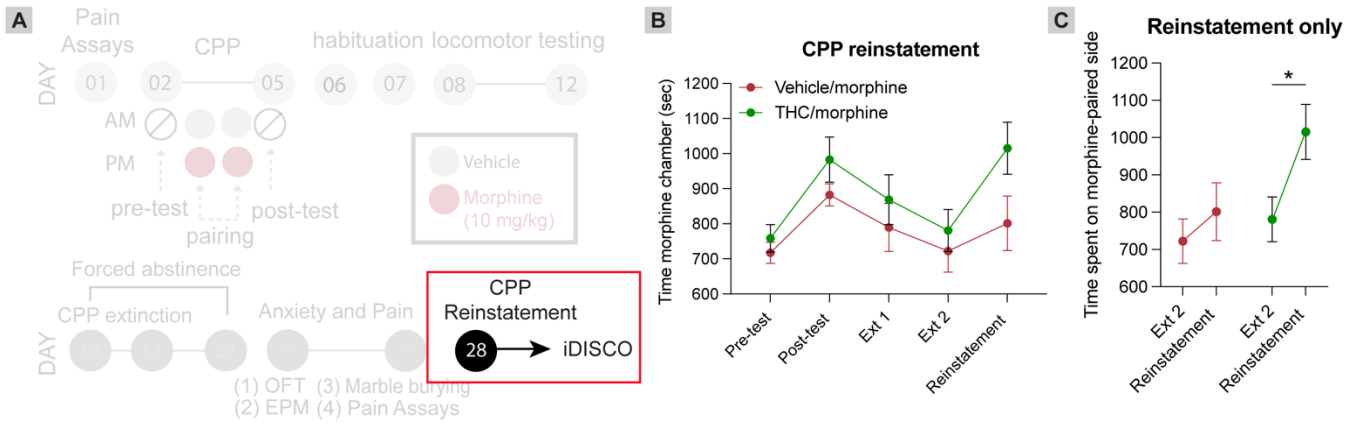

Figure 3: **Mice treated with THC during adolescence show an elevation in drug-induced reinstatement of morphine-seeking behaviors later in life**.

A, Timeline of experiments.

B, Time spent in the morphine-paired chamber during CPP pre-test, post-test, extinction, and reinstatement. Mice treated with THC or vehicle during adolescence showed a similar trajectory except for during reinstatement using a 5 mg/kg dose of morphine, at which time THC-treated mice showed an elevation in reinstatement behavior.

C, Quantification of the time spent in the morphine-paired chamber in the reinstatement task relative to the final extinction day. Vehicle/morphine-treated mice 722 s vs 801.3 s, = p = 0.43, n = 12 each; THC/morphine treated mice 780.7 s vs. 1015 s, p = 0.027, n = 8 each.

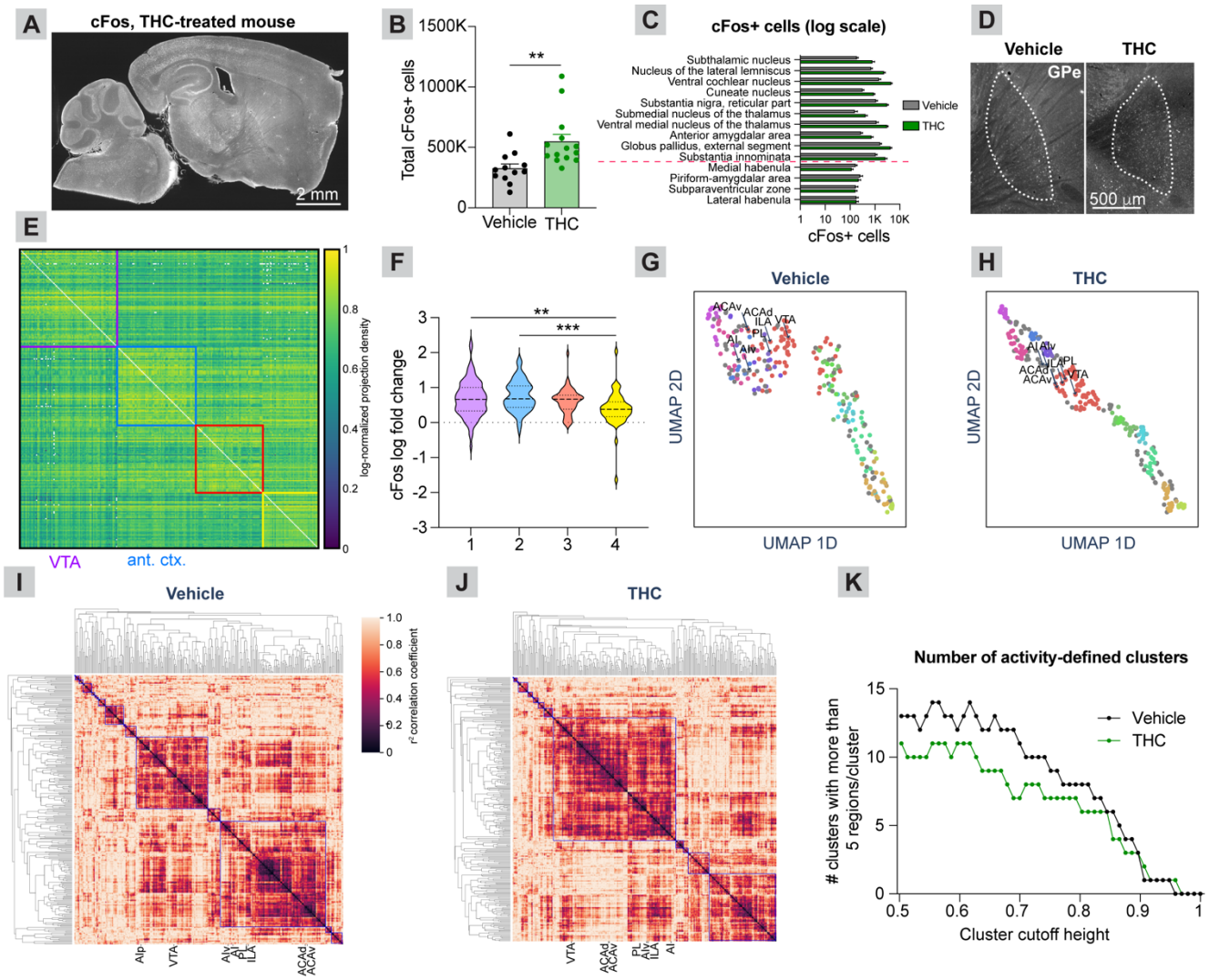

Figure 4: Brain-wide activity patterns in adolescent vehicle- and THC-treated mice following a reinstatement dose of morphine.

A, Representative sagittal section of a cFos-stained brain of an animal treated with THC during adolescence and following a reinstatement dose of morphine. Scale, 2 mm.

B, More cFos-expressing cells were detected in adolescent THC-treated mice than vehicle-treated mice following a reinstatement dose of 5 mg/kg morphine (548,481 vs. 325,789 cells, p = 0.0051).

C, The top ten brain regions showing the highest-fold elevation in cFos labeling in adolescent THC-treated relative to vehicle-treated mice and the four regions showing an elevation in vehicle-treated mice. Groups are separated by the dashed red line. Shown are brain regions with an average > 150 cFos+ cells in each brain regions.

D, Representative sagittal images of the GPe in adolescent vehicle-treated vs. THC-treated mice. Scale, 500 µm.

E, Anatomical connectivity matrix of the mouse brain, broken into four communities based on the Louvain method for community detection

588 **F**, Log fold-change in cFos labeling in each network community relative to one another (One-way ANOVA
589 p = 0.0002; purple (1) vs. blue (2) 0.68 vs. 0.75, p = 0.76; purple (1) vs. red (3) 0.68 vs. 0.61, p = 0.82;
590 purple (1) vs. yellow (4) 0.68 vs. 0.38, p = 0.0024; blue (2) vs. red (3) 0.75 vs. 0.61, p = 0.31; blue (2)
591 vs. yellow (4) 0.68 vs. 0.38, p = 0.0002; red (3) vs. yellow (4) 0.61 vs. 0.38, p = 0.05.
592 **G**, UMAP embedding of regions based on their correlated activity in adolescent vehicle-treated mice.
593 **H**, UMAP embedding of regions based on their correlated brain activity in adolescent THC-treated mice.
594 **I**, Hierarchical clustering of regions based on the cFos correlation matrix in adolescent vehicle-treated
595 mice.
596 **J**, Hierarchical clustering of regions based on the cFos correlation matrix in adolescent THC-treated
597 mice.
598 **K**, The number of hierarchical clusters in adolescent vehicle-treated and THC-treated mice across a
599 range of heights for cluster cut-offs in hierarchical trees.

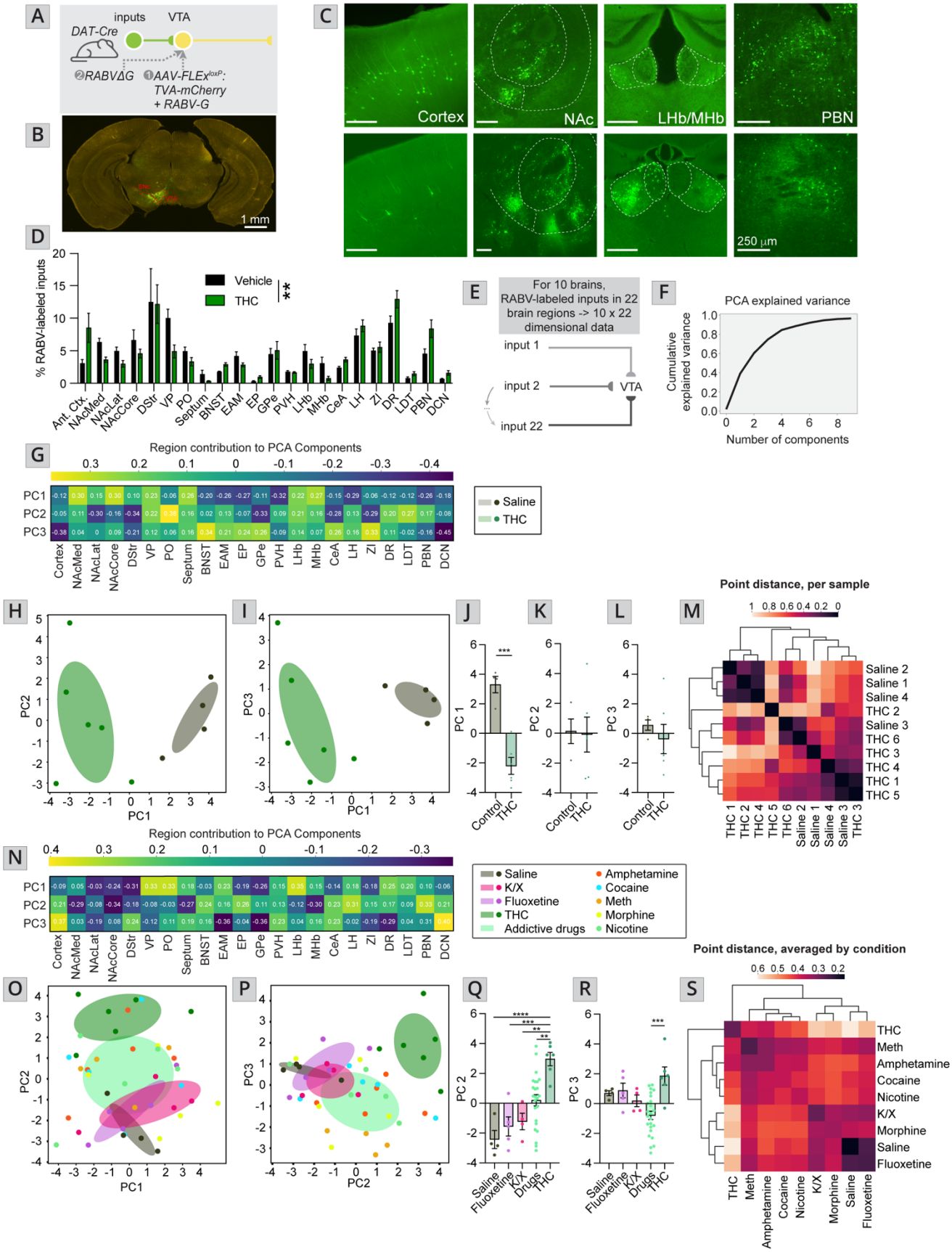

Figure 5: THC-treated mice show a different brain-wide pattern relative to animals treated with psychostimulants, opioids, or nicotine.

603 **A**, Schematic of experiments.
604 **B**, Representative image of the ventral midbrain of a DAT-Cre mouse showing starter cells in the VTA
605 and medial SNc. Scale, 1 mm.
606 **C**, Representative images of input cell populations in several brain sites, including the anterior cortex,
607 NAcMed, NAcCore, NAcLat, MHb, LHb, and PBN. Scale, 250 μm.
608 **D**, Bar graph plot showing the percentage of RABV-labeled inputs in control vs. THC-treated mice. Two-
609 way ANOVA, interaction $p = 0.0062$. Only the anterior cortex was significantly different following
610 correction for multiple comparisons (corrected p-value $p = 0.029$.
611 **E**, Schematic and explanation for how PCA analysis was carried out on the RABV tracing dataset.
612 **F**, Percent of cumulative variance explained by each principal component.
613 **G**, Heatmap of the contributions of each brain region, or feature, in the data to PCs 1 through 3.
614 **H**, Plot of PC1 and PC2 from brains of control and THC-treated mice.
615 **I**, Plot of PC1 and PC3 from brains of control and THC-treated mice.
616 **J-L**, Comparison of total PC values for each brain along **J** PC 1, **K** PC 2, and **L** PC 3. **J**, Control 3.3 vs.
617 THC -2.2, $p = 0.0002$. **K**, Control 0.13 vs. THC -0.09, $p = 0.89$. **L**, Control 0.57 vs. THC -0.38, $p = 0.48$.
618 **M**, To further quantify relationships between brains and conditions, the Euclidean distance between
619 each brain from control and THC-treated mice in the PC1 versus PC2 (or PC1 vs. PC3) coordinate
620 space was calculated. These distances were then plotted in a heatmap with brains being organized
621 by similarity assessed by hierarchical clustering.
622 **N**, Heatmap of the contributions of each brain region, or feature, in the data to PCs 1 through 3 in the
623 data presented in panels N-Q.
624 **O**, Plot of PC1 and PC2 from brains of control and drug-treated mice.
625 **P**, Plot of PC1 and PC3 from brains of control and drug-treated mice.
626 **Q-R**, Comparison of total PC values for each brain along **Q** PC 2, and **R** PC 3. For PC 1, One-way ANOVA
627 $p = 0.83$. **Q**, One-way ANOVA $p < 0.0001$; pairwise t-tests and asterisks presented in the figure include
628 THC comparisons only, although statistics are based on comparisons between all groups. Saline vs. THC
629 -2.43 vs. 2.96, $p < 0.0001$; Fluoxetine vs. THC -1.55 vs. 2.96, $p = 0.0004$; K/X vs. THC -1.23 vs. 2.96 p
630 $= 0.0024$; Drugs vs. THC 0.19 vs. 2.96, $p = 0.0051$. **R**, One-way ANOVA $p = 0.0004$; Saline vs. THC 0.70
631 vs. 1.85, $p = 0.63$; Fluoxetine vs. THC 0.88 vs. 1.85, $p = 0.71$; K/X vs. THC 0.19 vs. 1.85 $p = 0.27$; Drugs
632 vs. THC -0.79 vs. 1.85, $p = 0.0005$.
633 **S**, The Euclidean distance between each psychoactive drug-treated and control brain in the PC1 versus
634 PC2 coordinate space was calculated, plotted in a heatmap, and brains were organized by similarity and
635 assessed by hierarchical clustering.

REFERENCES:

1. National Center for Drug Abuse Statistics. Drug Abuse Statistics. (2024).

2. Hasin, D. S. *et al.* Prevalence of marijuana use disorders in the United States between 2001-2002 and 2012-2013. *JAMA Psychiatry* vol. 72 1235–1242 Preprint at https://doi.org/10.1001/jamapsychiatry.2015.1858 (2015).

3. Ferland, J. M. N. & Hurd, Y. L. Deconstructing the neurobiology of cannabis use disorder. *Nat Neurosci* **23**, 600–610 (2020).

4. Ruiz, C. M. *et al.* Pharmacokinetic, behavioral, and brain activity effects of ?9-tetrahydrocannabinol in adolescent male and female rats. *Neuropsychopharmacology* **46**, 959–969 (2021).

5. Chadwick, B., Miller, M. L. & Hurd, Y. L. Cannabis Use during Adolescent Development: Susceptibility to Psychiatric Illness. *Front Psychiatry* **4**, (2013).

6. Rubino, T., Zamberletti, E. & Parolaro, D. Adolescent exposure to cannabis as a risk factor for psychiatric disorders. *Journal of Psychopharmacology* vol. 26 177–188 Preprint at https://doi.org/10.1177/0269881111405362 (2012).

7. Panlilio, L. V., Zanettini, C., Barnes, C., Solinas, M. & Goldberg, S. R. Prior exposure to THC increases the addictive effects of nicotine in rats. *Neuropsychopharmacology* **38**, 1198–1208 (2013).

8. Stopponi, S. *et al.* Chronic THC during adolescence increases the vulnerability to stress-induced relapse to heroin seeking in adult rats. *European Neuropsychopharmacology* **24**, 1037–1045 (2014).

9. Lecca, D. *et al.* Adolescent cannabis exposure increases heroin reinforcement in rats genetically vulnerable to addiction. *Neuropharmacology* **166**, (2020).

10. Ellgren, M., Spano, S. M. & Hurd, Y. L. Adolescent cannabis exposure alters opiate intake and opioid limbic neuronal populations in adult rats. *Neuropsychopharmacology* **32**, 607–615 (2007).

11. Panlilio, L. V., Solinas, M., Matthews, S. A. & Goldberg, S. R. Previous exposure to THC alters the reinforcing efficacy and anxiety-related effects of cocaine in rats. *Neuropsychopharmacology* **32**, 646–657 (2007).

12. Friedman, A. L., Meurice, C. & Jutkiewicz, E. M. Effects of adolescent Δ9-tetrahydrocannabinol exposure on the behavioral effects of cocaine in adult Sprague–Dawley rats. *Exp Clin Psychopharmacol* **27**, 326–337 (2019).

13. Lüscher, C. & Malenka, R. C. Drug-Evoked Synaptic Plasticity in Addiction: From Molecular Changes to Circuit Remodeling. *Neuron* **69**, 650–663 (2011).

14. Rubino, T. *et al.* The Depressive Phenotype Induced in Adult Female Rats by Adolescent Exposure to THC is Associated with Cognitive Impairment and Altered Neuroplasticity in the Prefrontal Cortex. *Neurotox Res* **15**, 291–302 (2009).

15. Renard, J. *et al.* Adolescent Cannabinoid Exposure Induces a Persistent Sub-Cortical Hyper-Dopaminergic State and Associated Molecular Adaptations in the Prefrontal Cortex. *Cereb Cortex* **27**, 1297–1310 (2017).

16. Renard, J. *et al.* Adolescent THC Exposure Causes Enduring Prefrontal Cortical Disruption of GABAergic Inhibition and Dysregulation of Sub-Cortical Dopamine Function /631/378/2571 /631/378/1689/1799 /9 /9/30 /82 /82/1 article. *Sci Rep* **7**, (2017).

17. Creed, M. *et al.* Cocaine exposure enhances the activity of ventral tegmental area dopamine neurons via calcium-impermeable NMDARs. *Journal of Neuroscience* **36**, 10759–10768 (2016).

18. Bocklisch, C. *et al.* Cocaine Disinhibits Dopamine Neurons by Potentiation of GABA Transmission in the Ventral Tegmental Area. *Science (1979)* **341**, 1521–1525 (2013).

19. Beier, K. T. *et al.* Rabies screen reveals GPe control of cocaine-triggered plasticity. *Nature* **549**, 345–350 (2017).

20. Tian, G. *et al.* Molecular and circuit determinants in the globus pallidus mediating control of cocaine-induced behavioral plasticity. *Neuron Sneak Peek* (2023).

21. Cicero, T. J., Ellis, M. S., Surratt, H. L. & Kurtz, S. P. The changing face of heroin use in the United States a retrospective analysis of the past 50 years. *JAMA Psychiatry* **71**, 821–826 (2014).

22. Muhuri, P., Gfroerer, J. & Davies, M. *Substance Abuse and Mental Health Services Administration*. *Associations of Nonmedical Pain Reliever Use and Initiation of Heroin Use in the United States*. (2013).

23. Kandel, D. B. Marijuana Users in Young Adulthood. *Arch Gen Psychiatry* **41**, 200–209 (1984).

24. Clayton, R. & Voss, H. Young men and drugs in Manhattan: a causal analysis. *NIDA Res. Monogr.* **39**, 1–187 (1981).

25. O'Donnell, J. & Clayton, R. The stepping-stone hypothesis--marijuana, heroin, and causality. *Chem Depend.* **4**, 229–241 (1982).

26. Tanda, G., Pontieri, F. E. & Chiara, G. Di. *Cannabinoid and Heroin Activation of Mesolimbic Dopamine Transmission by a Common 1 Opioid Receptor Mechanism*. https://www.science.org.

27. Cadoni, C., Valentini, V. & Di Chiara, G. Behavioral sensitization to Δ9-tetrahydrocannabinol and cross-sensitization with morphine: Differential changes in accumbal shell and core dopamine transmission. *J Neurochem* **106**, 1586–1593 (2008).

28. Chaplan, S. R., Bach, F. W., Pogrel, J. W., Chung, J. M. & Yaksh, T. L. Quantitative assessment of tactile allodynia in the rat paw. *J Neurosci Methods* **53**, 55–63 (1994).

29. Renier, N. *et al.* IDISCO: A simple, rapid method to immunolabel large tissue samples for volume imaging. *Cell* **159**, 896–910 (2014).

30. Renier, N. *et al.* Mapping of Brain Activity by Automated Volume Analysis of Immediate Early Genes. *Cell* **165**, 1789–1802 (2016).

31. Oh, S. W. *et al.* A mesoscale connectome of the mouse brain. *Nature* **508**, 207–214 (2014).

32. Muller, B., Richards, A. J., Jin, B. & Lu, X. GOGrapher: A Python library for GO graph representation and analysis. *BMC Res Notes* **2**, (2009).

33. McInnes, L., Healy, J. & Melville, J. UMAP: Uniform Manifold Approximation and Projection for Dimension Reduction. *ArXiv* **1802.03426**, 1–51 (2018).

34. McInnes, L., Healy, J. & Astels, S. hdbscan: Hierarchical density based clustering. *The Journal of Open Source Software* **2**, 205 (2017).

35. Waskom, M. Seaborn: Statistical Data Visualization. *J Open Source Softw* **6**, 3021 (2021).

36. Beier, K. T. *et al.* Circuit Architecture of VTA Dopamine Neurons Revealed by Systematic Input-Output Mapping. *Cell* **162**, 622–634 (2015).

37. Kubilius, R. A., Kaplick, P. M. & Wotjak, C. T. Highway to hell or magic smoke? The dose-dependence of Δ 9 -THC in place conditioning paradigms. in *Learning and Memory* vol. 25 446–454 (Cold Spring Harbor Laboratory Press, 2018).

38. Bartas, K. *et al.* Drug-induced changes in connectivity to midbrain dopamine cells revealed by rabies monosynaptic tracing. *Elife* **13**, RP93664 (2024).

39. Derdeyn, P., Hui, M., Macchia, D. & Beier, K. Uncovering the Connectivity Logic of the Ventral Tegmental Area. *Front Neural Circuits* **15**, 799688 (2022).

40. Nielsen, S. *et al.* Opioid-sparing effect of cannabinoids: A systematic review and meta-analysis. *Neuropsychopharmacology* vol. 42 1752–1765 Preprint at https://doi.org/10.1038/npp.2017.51 (2017).

41. Ellgren, M., Spano, S. M. & Hurd, Y. L. Adolescent cannabis exposure alters opiate intake and opioid limbic neuronal populations in adult rats. *Neuropsychopharmacology* **32**, 607–615 (2007).

42. Levin, E. D., Rezvani, A. H., Montoya, D., Rose, J. E. & Scott Swartzwelder, H. Adolescent-onset nicotine self-administration modeled in female rats. *Psychopharmacology (Berl)* **169**, 141–149 (2003).

43. Faraday, M. M., Elliott, B. M. & Grunberg, N. E. *Adult vs. Adolescent Rats Differ in Biobehavioral Responses to Chronic Nicotine Administration*. www.elsevier.com/locate/pharmbiochembeh.

44. Vastola, B. J., Douglas, L. A., Varlinskaya, E. I. & Spear, L. P. *Nicotine-Induced Conditioned Place Preference in Adolescent and Adult Rats*.

45. Faraday MM, Elliott BM, Phillips JM & Grunberg NE. Adolescent and adult male rats differ in sensitivity to nicotine's activity effects. *Pharmacol Biochem Behav.* **74**, 917–931 (2003).

46. O'Dell, L. E., Bruijnzeel, A. W., Ghozland, S., Markou, A. & Koob, G. F. Nicotine withdrawal in adolescent and adult rats. in *Annals of the New York Academy of Sciences* vol. 1021 167–174 (New York Academy of Sciences, 2004).

47. Carpenter, M. D., Manners, M. T., Heller, E. A. & Blendy, J. A. Adolescent oxycodone exposure inhibits withdrawal-induced expression of genes associated with the dopamine transmission. *Addiction Biology* **26**, (2021).

48. Wickersham, I. R. *et al.* Monosynaptic Restriction of Transsynaptic Tracing from Single, Genetically Targeted Neurons. *Neuron* **53**, 639–647 (2007).

49. Wall, N. R., Wickersham, I. R., Cetin, A., De La Parra, M. & Callaway, E. M. Monosynaptic circuit tracing in vivo through Cre-dependent targeting and complementation of modified rabies virus. *Proc Natl Acad Sci U S A* **107**, 21848–21853 (2010).

50. Tian, G. *et al.* An extended Amygdala-midbrain circuit controlling cocaine withdrawal-induced anxiety and reinstatement. *Cell Rep* **39**, 1–16 (2022).

51. Koob, G. F. & Volkow, N. D. Neurocircuitry of addiction. *Neuropsychopharmacology* **35**, 217–238 (2010).

52. Goldstein, R. Z. & Volkow, N. D. Dysfunction of the prefrontal cortex in addiction: Neuroimaging findings and clinical implications. *Nat Rev Neurosci* **12**, 652–669 (2011).

53. Volkow, N. D., Michaelides, M. & Baler, R. The neuroscience of drug reward and addiction. *Physiol Rev* **99**, 2115–2140 (2019).

54. Miller, E. K. & Cohen, J. D. AN INTEGRATIVE THEORY OF PREFRONTAL CORTEX FUNCTION. *Annu. Rev. Neurosci* **24**, 167–202 (2001).